

RUTHENIUM (II) SCHIFF BASE: COMPLEXES, PHYSICO-CHEMICAL, SPECTROMETRIC, MICROBIAL AND DNA BINDING AND CLEAVING STUDIES

S. Arunachalam^a, N. Padma Priya^a, C. Jayabalakrishnan^b, and V. Chinnusamy^{b*},

^aDepartment of Chemistry, Kongunadu college of Arts and Science College, Coimbatore – 641029, India.

^bPost Graduate and Research Department of Chemistry, Sri Ramakrishna Mission Vidyalaya College of Arts and Science, Coimbatore – 641020, India.

ABSTRACT: Stable ruthenium(II) carbonyl complexes having the general composition $[\text{Ru}(\text{CO})(\text{PPh}_3)(\text{py})(\text{L})]$ (where L= biantion of tridentate Schiff bases (H_2L^1 , H_2L^2 and H_2L^3)) were synthesized from the reaction of $[\text{RuHCl}(\text{CO})(\text{PPh}_3)_2(\text{py})]$ with bidentate Schiff base ligands derived from condensation of isatin with *o*-aminophenol / *o*-aminothiophenol / *o*-aminobenzoic acid. The new complexes were characterized by elemental analysis, Mass spectra, IR, UV-Vis and ^1H , ^{13}C and ^{31}P - NMR spectral data. The redox property of the complexes were studied by cyclic voltammetric technique. An octahedral geometry has been assigned tentatively for all the complexes. In all the above reactions, the Schiff bases replaces a hydride and chloride ion and PPh_3 from the starting complexes, which indicate that the Ru–N bonds present in the complexes containing heterocyclic nitrogen bases are stronger than the Ru–P. These complexes were also subjected to study their biocidal activity against *S. epidermidis* and *E. coli*. Some of the complexes show higher efficiency when compared with the standard (*Ciprofloxacin* and *Co-trimoxazole*). DNA (*Herring Sperm*) binding behaviour of the complex $[\text{Ru}(\text{L}^1)(\text{CO})(\text{PPh}_3)(\text{py})]$ has been studied by electronic spectra, cyclic voltammetric, differential pulse voltametric (DPV), circular dichorism and gel electrophoresis techniques.

Key words: Schiff base; ruthenium(II) DNA binding

INTRODUCTION

Interaction of metal ions with N, O and S containing organic moieties has attracted much attention in recent years [1,2]. Such ligands and their complexes have become important due to their biological activity [3-5] and also because they provide a better understanding of metal protein binding [6]. Thus, Schiff bases containing these groups could act as a versatile model of metallic biosites [7]. For the synthesis of model compounds, dibasic tridentate ligands proved to be especially favourable [8]. Interest in transition metal complexes of these Schiff bases continues not only due to the interesting structural and bonding modes they possess, but also because of their various industrial applications [9]. There has been a remarkable interest in the synthesis and study of unsymmetrical Schiff base complexes with transition metal cations [10–15], arising from the awareness that the resulting complexes may serve as models of relevance to bio-inorganic chemistry such as metalloproteins and metalloenzymes [16–20] in which transition metals are bound to a macrocycle, such as a heme ring, or to donor atoms of peptide chains, usually in a distorted environment. Asymmetric complexes are proposed as convenient models for irregular metal ion binding to peptides [21–24]. DNA is the primary target for most anticancer and antiviral therapies according to cell biology. Investigation of the interaction of DNA with small molecules is a basic study in the design of new type of pharmaceutical molecules. When some kinds of metal complexes [25] interact with DNA, they could induce the breakage of DNA strands by appropriate ways. Thus, to cancer genes, after DNA strand are cleaved by metal complexes and other cleaving agents, the DNA double strand break. In recent years, binding studies of transition metal complexes have become very important in the development of DNA molecule probes and chemotherapy [26-31]. These complexes can bind to DNA in non-covalent modes such as electrostatic, intercalative or groove binding. For an intercalative interaction the planar aromatic heterocyclic group inserts and stacks between the base pair of DNA. In this paper, we discuss the tridentate Schiff base ruthenium(II) carbonyl complexes: Physico-chemical, spectrometric, microbial, DNA binding and cleavage studies.

*Corresponding Author.

Email id : drvcsrkv@gmail.com (V. Chinnusamy)

Physical Measurements

Melting Points

Melting points were recorded on a Veego VMP-DS melting point apparatus and are uncorrected.

Elemental analyses

The analysis of carbon, hydrogen, nitrogen and sulphur were performed in Vario EL III CHNS analyzer at Cochin University, Kerala, India.

IR spectra

IR spectra were recorded as KBr pellets in the 400 - 4000 cm^{-1} region using a Perkin Elmer FT-IR 8000 spectro-photometer with a resolution of 4 cm^{-1} in transmittance mode.

UV-Vis spectra

Electronic spectra of all ligands and the complexes were taken in dichloromethane solution in quartz cells. The concentration of the complexes ranges around 0.02 – 0.3N. The spectra were recorded on a Systronics double beam UV-Vis Spectrophotometer 2202 in the range 200-800 nm at room temperature.

NMR spectra

^1H and ^{13}C -NMR spectra for the ligands and complexes were recorded using Bruker 500 MHz instrument in CDCl_3 at room temperature in Indian Institute of Science, Bangalore. Minimum quantities of ligands and complexes were dissolved in deuterated CDCl_3 . ^1H -NMR chemical shifts were referenced to tetramethylsilane (TMS) as an internal solvent standard resonance and ^{13}C -NMR chemical shifts were referenced to the internal solvent resonance. ^{31}P -NMR spectra of the complexes were obtained at room temperature using *o*-phosphoric acid as a reference. Signals are quoted in parts per million as δ downfield from internal reference.

Cyclic voltammetry

Cyclic voltammetric studies were carried out in acetonitrile using a glassy-carbon working electrode and potentials were referenced to standard calomel electrode at Madurai Kamaraj University, Madurai. Minimum quantity of the complexes was dissolved in acetonitrile and decimolar solution of TPAP was added.

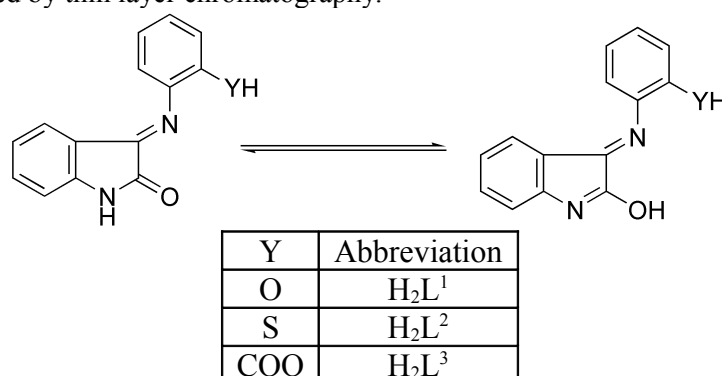
Methods

The starting complex $\text{RuHCl}(\text{CO})(\text{py})(\text{PPh}_3)$ [32] and tridentate Schiff base ligands [2] were prepared according to the literature procedures. Microbial studies [2] were carried out according to reported procedures and DNA binding studies by titration method [28].

Recommended procedures

Synthesis of new Schiff base ligands

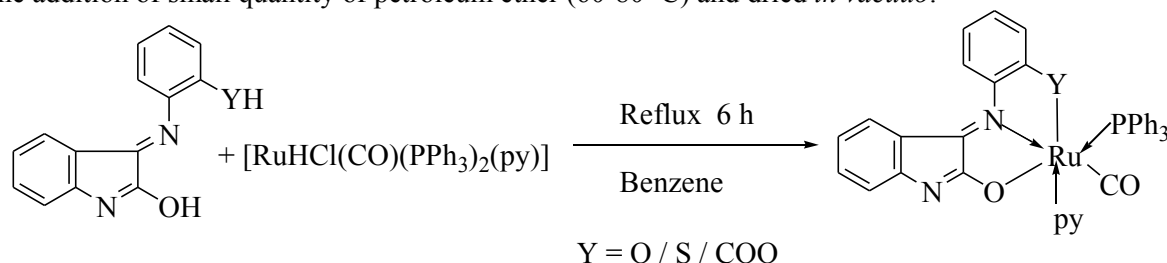
To an ethanolic solution of isatin (0.1 m mol) with *o*-aminophenol (0.1 m mol)/*o*-aminothiophenol (0.1 m mol)/ *o*-aminobenzoic acid (0.1 m mol) was added in 1:1 molar ratio and the mixture was stirred about for half an hour. The above solution was refluxed for 6 hours (Scheme 1). The resulting solution was concentrated and the product obtained was washed with ethanol and their purity of the ligands were checked by thin layer chromatography.



Scheme.1 Keto-enol tautomerism of the new Schiff base ligands

Synthesis of new Ru(II) Schiff base complexes

All the new complexes were prepared by the following general procedure as described below (Scheme 2). To a solution of $[\text{RuHCl}(\text{CO})(\text{PPh}_3)_2(\text{py})]$ (0.1mmol) in benzene (20 cm^3) the appropriate Schiff base (0.1 mmol) was added in 1:1 molar ratio and heated under reflux for 6 hours. The resulting solution was then concentrated to 3 cm^3 and cooled. The complex was precipitated by the addition of small quantity of petroleum ether (60-80 $^\circ\text{C}$) and dried *in vacuo*.



Scheme 2. Preparation of new Ru(II) Schiff base complexes

RESULTS AND DISCUSSION

Stable ruthenium(II) Schiff base complexes of the general formula $[\text{Ru}(\text{L})(\text{CO})(\text{PPh}_3)(\text{py})]$ (where L = bianion tridentate Schiff base) have been prepared by reacting $[\text{RuHCl}(\text{CO})(\text{PPh}_3)(\text{py})]$ with the respective Schiff bases in a 1:1 molar ratio in benzene (Scheme 2). All the complexes are soluble in most of the common organic solvents. Their purity was checked by TLC on silica gel. The analytical data obtained for the new complexes agree well with the proposed molecular formula (Table 1). In all of the above reactions, the Schiff bases behave as binegative tridentate ligands.

Table 1. Analytical data of Ru(II) Schiff base complexes

Complexes	Colour	M.p. ($^\circ\text{C}$)	Empirical formula	Molecular weight	Elemental analysis Calculated (found) (%)			
					C	H	N	S
$[\text{Ru}(\text{L}^1)(\text{CO})(\text{PPh}_3)(\text{py})]$	Brown	217	$\text{C}_{38}\text{H}_{29}\text{N}_3\text{O}_3\text{PRu}$	707.70	64.49(64.43)	4.13(4.09)	5.94(5.89)	-
$[\text{Ru}(\text{L}^2)(\text{CO})(\text{PPh}_3)(\text{py})]$	Brown	193	$\text{C}_{38}\text{H}_{29}\text{N}_3\text{O}_2\text{PSRu}$	724.08	63.06(62.98)	4.04(4.01)	5.81(5.79)	4.41(4.39)
$[\text{Ru}(\text{L}^3)(\text{CO})(\text{PPh}_3)(\text{py})]$	Green	189	$\text{C}_{39}\text{H}_{29}\text{N}_3\text{O}_4\text{PRu}$	735.71	63.67(63.61)	3.97(3.91)	5.71(5.68)	-

Mass spectrometry

The mass spectra of $[\text{Ru}(\text{CO})(\text{PPh}_3)(\text{py})(\text{L}^1)]$, $[\text{Ru}(\text{CO})(\text{PPh}_3)(\text{py})(\text{L}^2)]$ and $[\text{Ru}(\text{CO})(\text{PPh}_3)(\text{py})(\text{L}^3)]$ displayed the molecular ion isotopic peak at m/z 707.6989, 723.7645 and 735.7097 respectively and the remaining peaks represents the successive degradation of the complexes. These peaks are consistent with the proposed molecular formula of the corresponding ruthenium(II) Schiff base complexes.

SPECTROSCOPIC STUDIES

Infrared spectral analysis

The IR spectra of the ligands were compared with those of the ruthenium complexes in order to confirm the binding mode of the Schiff base ligands to the ruthenium atom in the complexes (Table 2). The free Schiff base ligands showed a strong band in the region 1615-1617 cm^{-1} , which is characteristic of the azomethine $\nu_{(\text{C}=\text{N})}$ group. Coordination of the Schiff bases to the metal through the nitrogen atom is expected to reduce the electron density in the azomethine link and lower the $\nu_{(\text{C}=\text{N})}$ absorption frequency.

Table 2. FT-IR spectral and UV-Vis data of new Ru (II) Schiff base complexes

Complexes	IR spectra (cm ⁻¹)						UV-Vis λ _{max} (nm)
	ν _{C=N}	ν _{C-O}	ν _{C-S}	ν _{asy (COO⁻)}	ν _{sym (COO⁻)}	ν _{C=O}	
[Ru(L ¹)(CO)(PPh ₃)(py)]	1594	1434	-	-	-	1941	256, 298, 349, 398, 462
[Ru(L ²)(CO)(PPh ₃)(py)]	1589	-	126	-	-	1967	258, 301, 366, 389, 451
[Ru(L ³)(CO)(PPh ₃)(py)]	1596	-	-	1695	1482	1956	258, 299, 350, 408, 440, 440, 461

The band due to ν_(C=N) is shifted to lower frequencies and appears around 1589-1596 cm⁻¹, indicating coordination of the azomethine nitrogen to the ruthenium metal [2,33]. A strong band observed at 1343 cm⁻¹ in the free Schiff base H₂L¹ has been assigned to phenolic C–O stretching. On complexation, this band is shifted to a higher frequency at 1434 cm⁻¹, indicating coordination through the phenolic oxygen. This has been further supported by the disappearance of the broad band ν_(OH) around 3000 cm⁻¹ in the complex [Ru(CO)(PPh₃)(py)(L¹)], indicating deprotonation of the phenolic proton prior to coordination [2,33]. In the IR spectra of the Schiff base H₂L², a very weak absorption band appeared at 2834 cm⁻¹ corresponding to ν_(S-H) disappeared in the spectra of the complexes due to the fact that coordination takes place through the sulphur atom after deprotonation. Moreover, the absorption due to ν_(C-S) of the ligand at 1224 cm⁻¹ is shifted to a higher frequency at 1261 cm⁻¹ in the complex [Ru(CO)(PPh₃)(py)(L²)], indicating that the other coordination is through thiophenolic sulphur atom [2,33]. For the *o*-aminobenzoic acid moiety, the free Schiff base H₂L³ shows the ν_(O-H) absorption observed at 3300cm⁻¹ and the ν_(C=O) frequency of the carbonyl was seen as a band at 1731 cm⁻¹ and also shows the absorption bands in the 1681 cm⁻¹ and 1485 cm⁻¹ regions for asymmetric ν_(COO⁻) and symmetric ν_(COO⁻) stretching. In the complex [Ru(CO)(PPh₃)(py)(L³)], the bands were observed in the 1695 cm⁻¹ and 1482 cm⁻¹ regions arising from asymmetric ν_(COO⁻) and symmetric ν_(COO⁻) stretching of the carboxylato group.^[2,35] This indicates the coordination of the carboxyl group to ruthenium metal ion in the complexes. The differences between the asymmetric and symmetric stretching frequencies of the coordinated carboxyl group lie in the 213 cm⁻¹ range, a clear indication of the monodentate coordination of the carboxyl group with that of free carbonyl group [2,33]. The characteristic bands due to triphenylphosphine were observed in the expected region. The characteristic band for ν_(C=O) and ν_(NH) disappears on complexation [34]. This may be due to the enolisation and subsequent coordination through the deprotonated oxygen atom [34]. In the entire complexes strong band appears in the region 1941-1967 cm⁻¹ owing to terminal carbonyl group. In all the complexes, a medium intensity band is observed in the 1091-1093 cm⁻¹ region characteristic of the coordinated pyridine [35].

Electronic spectral analysis

The electronic spectra of all the complexes in dichloromethane showed five to seven bands in the 256-462 nm regions (Table 2). The electronic spectra of all the complexes showed two types of transitions, the first one appeared at range 256-301 nm which can be assigned to π-π* transition due to transitions involving molecular orbitals located on the phenolic, thiophenolic and carboxylic chromophore. This reveals that one of the coordination site is oxygen of the phenolic and carboxylic and sulphur of the thiophenolic groups respectively. The second type of transitions appeared at range 349-462 nm assigned to n→π* transition due to azomethine groups and benzene ring of the ligands. These bands have also been shifted in the spectra of the new complexes indicating the involvement of imine group nitrogens in coordination with central metal atom. All the complexes are diamagnetic, indicating the presence of ruthenium in the +2 oxidation state. The ground state of ruthenium(II) in an octahedral environment is ¹A_{1g}, arising from the t_{2g}⁶ configuration. The excited state terms are ³T_{1g}, ³T_{2g}, ¹T_{1g} and ¹T_{2g}. Hence four bands corresponding to the transition ¹A_{1g}→³T_{1g}, ¹A_{1g}→³T_{2g}, ¹A_{1g}→¹T_{1g} and ¹A_{1g}→¹T_{2g} are possible in order of increasing energy. The other high intensity band in the visible region around 256–462 nm has been assigned to charge transfer transitions arising from the metal t_{2g} level to the unfilled π* molecular orbital of the ligand [36-40]. The pattern of the electronic spectra for all the complexes indicate the presence of an octahedral environment around the ruthenium(II) ion similar to that of other ruthenium octahedral complexes [36-41].

¹H -NMR Spectra of Ru(II) Schiff base complexes

The ¹H - NMR spectra of all the complexes were recorded to confirm the binding of Schiff bases to the ruthenium ion shown in the Table 3. Multiplets are observed around 6.5–7.9 ppm in all the complexes have been assigned to aromatic protons of triphenylphosphine, pyridine and Schiff base ligands [42,43]. A sharp singlet observed for Ph-OH, Ph-SH, Ph-COOH and enolic-OH protons for all the ligands were disappeared in all the complexes which indicates the coordination of ruthenium through the Ph-O, Ph-S, Ph-COO [44,45] and enolic-O atoms [34]

¹³C -NMR Spectra of Ru(II) Schiff base complexes

The ¹³C NMR data for the complexes [Ru(CO)(PPh₃)(py)(L¹)], [Ru(CO)(PPh₃)(py)(L²)] and [Ru(CO)(PPh₃)(py)(L³)] have been recorded and the values are tabulated in the Table 3. The chemical shifts for the aromatic carbon atoms triphenylphosphine of the complexes appears at 108-137 ppm. In all the complexes, Ph-C-O, Ph-C-S and Ph-C-COO appears at 138, 133 and 164 ppm respectively and also for Ph-C=N-Ph and Ph-N=C-O in the complexes appears in the range 134-159 ppm and 159-181 ppm respectively. For all the complexes, the terminal carbonyl group C≡O appears in the range 181-184 ppm respectively.

³¹P -NMR Spectra of the Ru(II) complexes

³¹P-NMR spectra were recorded for all the complexes in order to confirm the presence of triphenylphosphine group. For the complexes [Ru(L¹)(CO)(PPh₃)(py)], [Ru(L²)(CO)(PPh₃)(py)] and [Ru(L³)(CO)(PPh₃)(py)] peak appears at 26.46, 26.91 and 28.09 ppm respectively, indicates the presence of only one triphenylphosphine [46].

Electrochemistry

Complexes were electrochemically examined at a glass carbon working electrode in dichloromethane solution using cyclic voltammetry (Table 4). The oxidation and reduction of each complex were characterized by well defined waves with E_f values in the range from -0.695 to -0.75 mV (reduction) against Ag/AgCl electrode and there is no potential observed for oxidation. Complexes showed reduction couples with peak to peak separation values (ΔE_p) ranging from 340 to 480 mV revealing that this process is at best quasi-reversible. This is attributed to slow electron transfer and adsorption of the complex on to the electrode surface. The reduction potential of Ru(II) complexes are affected by chelate rings of the ligands and it is observed that the reduction potential of complexes with a larger chelate ring is more than that of complexes with a smaller chelate ring. It has also been observed from the electrochemical data that there is not much variation in the redox potential due to triphenylphosphine and pyridine [36-38].

Table 3. NMR Spectral data of Ru(II) Schiff base complexes

Complexes	¹ H-NMR (ppm)	¹³ C-NMR (ppm)	³¹ P-NMR(ppm)
[Ru(L ¹)(CO)(PPh ₃)(py)]	6.7-7.6 (m,aromatic)	110, 115, 118, 123, 128, 129, 137 (aromatic C), 138 (Ph-C-O), 151 (Ph-C=N-Ph), 159 (Ph-N=C-O), 184.86 (Ru-C≡O)	26.46
[Ru(L ²)(CO)(PPh ₃)(py)]	6.5-7.6 (m,aromatic)	108, 119, 122, 126, 129, 130, 131, 132 (aromatic C), 133 (Ph-C-S), 134 (Ph-C=N-Ph), 141 (Ph-N=C-O), 181 (Ru-C≡O)	26.91
[Ru(L ³)(CO)(PPh ₃)(py)]	6.7-7.6 (m,aromatic)	111,116, 119, 122, 125, 128, 129, 130 (aromatic C), 164 (Ph-C-COO), 134 (Ph-C=N-Ph), 174 (Ph-N=C-O), 182 (Ru-C≡O)	28.09

Table 4. Electrochemistry data of new Ru(II) Schiff base complexes

Complexes	Ru ^{II} - Ru ^I			
	E _{pa} (V)	E _{pc} (V)	E _f (V)	ΔE _p (mV)
[Ru(L ¹)(CO)(PPh ₃)(py)]	-0.58	-0.92	-0.75	340
[Ru(L ²)(CO)(PPh ₃)(py)]	-0.5	-0.92	-0.74	480
[Ru(L ³)(CO)(PPh ₃)(py)]	-0.48	-0.91	-0.695	430

Supporting electrolyte: [NBu₄]ClO₄ (0.1M); Scan rate, 0.1 mV⁻¹; reference electrode, Ag-AgCl. ΔE_p = E_{pa} - E_{pc}; E_{1/2} = 0.5 (E_{pa} + E_{pc}), Where E_{pa} and E_{pc} are the anodic and cathodic peak potentials in Volts, respectively.

Microbial Studies

The *in vitro* cytotoxicity of ligands and the complexes were screened in order to evaluate activity against *Staphylococcus epidermidis* and *Escherichia coli* at 0.25 %, 0.50 % and 1 % concentration and the results are shown in Table 5. From the results it is inferred that the ruthenium(II) Schiff base complexes show higher efficiency when compared with the standard (*Ciprofloxacin*), parent ligands, ruthenium(II) precursor against same microbes under identical experimental conditions. This would suggest that the chelation could facilitate the ability of a complex to cross a cell membrane [47] and can be explained by Tweedy's chelation theory [48] Chelation considerably reduces the polarity of the metal ion because of partial sharing of its positive charge with donor groups and possible π -electron delocalization over the whole chelate ring. Such a chelation could enhance the lipophilic character of the central metal atom, which subsequently favours its permeation through the lipid layer of the cell membrane. This increased lipophilicity enhances the penetration of the complexes into lipid membrane and blocking the metal binding sites on enzymes of microorganism. These complexes also disturb the respiration process of the cell and thus block the synthesis of proteins which restrict the further growth of the organism [47,48] The variation in the effectiveness of different compounds against different organisms depends either on the impermeability of the cells of the microbes or on differences in ribosome of microbial cells.

Table 5. Biocidal activity of new Ru(II) Schiff base complexes

Complexes	Diameter of inhibition zone (mm)					
	<i>S. epidermidis</i>			<i>E. coli</i>		
	0.25%	0.5%	1.0%	0.25%	0.5%	1.0%
[Ru(L ¹)(CO)(PPh ₃)(py)]	22	22	22	21	23	23
[Ru(L ²)(CO)(PPh ₃)(py)]	28	28	29	29	29	30
[Ru(L ³)(CO)(PPh ₃)(py)]	27	27	27	26	27	27
Standard	<i>Ciprofloxacin</i> (22)					

DNA binding and cleavage studies

Electronic absorption titration

Electronic absorption spectroscopy is one of the most powerful experimental techniques for probing metal ion–DNA interactions. Binding of the macromolecule leads to changes in the electronic absorption spectrum of the metal complex. Base binding is expected to perturb the ligand field transition of the metal complex. Intercalative mode of binding usually results in hypochromism and bathochromism due to the strong stacking interaction between an aromatic chromophore and the base pairs of DNA. The extent of hypochromism parallels the strength of intercalative binding. On the other hand, metal complexes, which bind non-intercalatively or electrostatically with DNA, may result in hyperchromism or hypochromism [49-51].

The electronic absorption titration of complex [Ru(CO)(L¹)(py)(PPh₃)] has been carried out at a fixed concentration of complexes (100 μ M) in aqueous media at 25 °C, while varying the concentration of DNA (0-150 μ M). The absorption spectra of the complex [Ru(CO)(L¹)(py)(PPh₃)] in the absence and presence of DNA is depicted in the Figure 1 (Table 6). Addition of increasing amount of DNA results in an appreciable decrease in absorption intensity of LMCT band at 392 nm with insignificant shift in wavelength. The complex [Ru(CO)(L)(py)(PPh₃)] showed hypochromism (24%) and the K_b value is $2.1 \times 10^4 \text{ M}^{-1}$. Isosbestic points are observed near 292 nm for [Ru(CO)(L¹)(py)(PPh₃)], while binding to DNA, suggesting that the complex has a single mode of binding to DNA [52]. Determinations of intrinsic binding constant, K_b , based upon these absorption titrations may be made with the following equation [53]:

$$[\text{DNA}] / (\epsilon_A - \epsilon_F) = [\text{DNA}] / (\epsilon_B - \epsilon_F) + 1/K_b (\epsilon_B - \epsilon_F)$$

Table 6. Electrochemical behaviour of complex $[\text{Ru}(\text{L}^1)(\text{CO})(\text{PPh}_3)(\text{py})]$ on interaction with DNA in Tris-HCl buffer

R	E_{pa}/V	E_{pc}/V	$\Delta E_p(\text{V})$	i_{pa}/i_{pc}	$E^*_{1/2}(\text{V})$	$\Delta E_{1/2}(\text{V})$	K_{1+}/K_{2+}
0	-0.094	-0.703	0.609	0.342	-0.591	-	-
0.2	-0.091	-0.692	0.601	0.481	-0.587	0.004	1.17
0.4	-0.053	-0.774	0.621	0.502	-0.571	0.020	2.18
0.6	-0.022	-0.651	0.629	0.540	-0.563	0.028	2.98

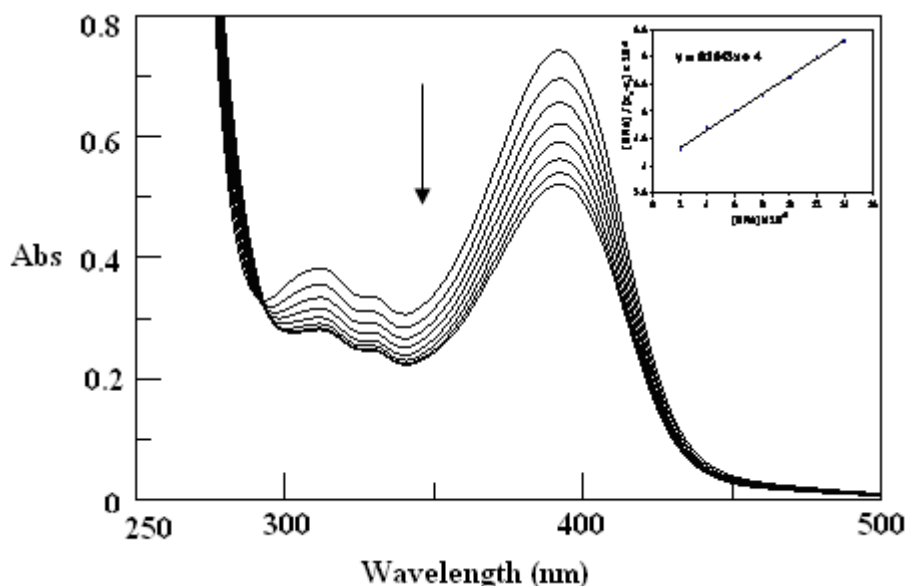


Fig. 1. Absorption spectra of $[\text{Ru}(\text{CO})(\text{L}^1)(\text{py})(\text{PPh}_3)]$ complex ($100 \mu\text{M}$) in aqueous Tris buffer (5 mM tris HCl, 50 mM NaCl, pH 7.1) upon the addition of herring sperm DNA. ($0\text{-}100 \mu\text{M}$.)

Arrow shows the absorbance change upon the increase of DNA concentration where ϵ_A , ϵ_F , and ϵ_B correspond to $A_{\text{obsd}}/[\text{complex}]$, the extinction coefficient for the free complex and the extinction coefficient for the complex in the fully bound form, respectively. The slope and y intercept of the linear fit of $[\text{DNA}]/(\epsilon_A - \epsilon_F)$ versus $[\text{DNA}]$ give $1/(\epsilon_B - \epsilon_F)$ and $1/K_b(\epsilon_B - \epsilon_F)$ respectively. The intrinsic binding constant, K_b can be obtained from the ratio of slope to the intercept. The K_b values observed here are lower than those observed for typical classical intercalators (ethidium-DNA, $7.0 \times 10^7 \text{ M}^{-1}$ in 40 mM Tris-HCl buffer, pH 7.9 [54], and $1.4 \times 10^6 \text{ M}^{-1}$ in 40 mM NaCl- 25 mM Tris-HCl [55]; proflavin with *Escherichia coli* DNA, 50% GC content, $4.1 \times 10^5 \text{ M}^{-1}$ in 0.1 M Tris-HCl) [56] with a proven DNA-binding mode involving the complete insertion of the planar molecules between the base pairs. This is indicative of binding of the complex $[\text{Ru}(\text{CO})(\text{L}^1)(\text{py})(\text{PPh}_3)]$ with DNA host with lower affinity than the classical intercalators.

Cyclic voltammetry

Electrochemical methods are widely used to study the interaction of DNA with metal chelates. Based on the shift of potential in the cyclic voltammograms, the interaction mode of compounds with DNA can be inferred [57] (Fig 2 and 3). The application of cyclic voltammetry (CV) and differential pulse voltammetry (DPV) to the study of binding of metal complexes to DNA provides a useful complement to the methods of investigations such as UV-visible (UV-Vis) and circular dichroism (CD) spectroscopies [58,59]. For the complex $[\text{Ru}(\text{CO})(\text{L}^1)(\text{py})(\text{PPh}_3)]$ the separation of anodic and cathodic peak potentials, ΔE_p is large and the ratio of anodic to cathodic peak currents, i_{pa}/i_{pc} is less than unity, indicating quasi-reversible one electron redox process in complex $[\text{Ru}(\text{CO})(\text{L}^1)(\text{py})(\text{PPh}_3)]$ (Table 6). Since Ru(II)/Ru(I) couples are irreversible as shown by the large ΔE_p values even at $R = 0$ ($R = [\text{DNA}]/[\text{complex}]$), no attempt was made to calculate the binding constant from CV.

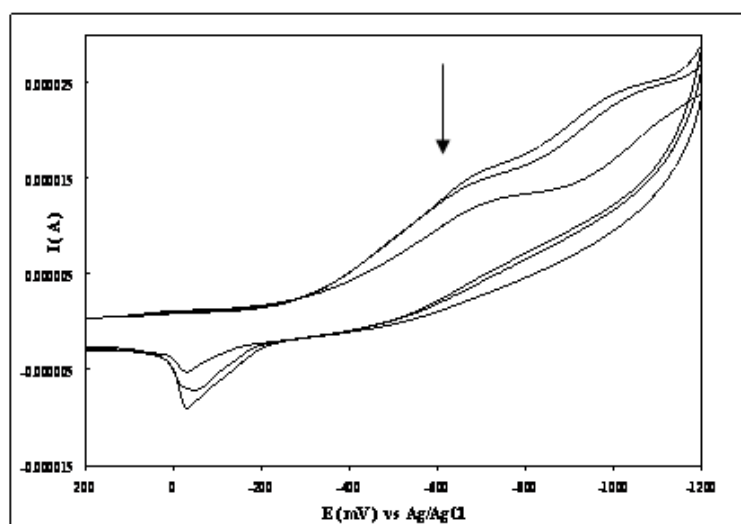


Fig. 2. Cyclic voltammograms of $[\text{Ru}(\text{CO})(\text{L}^1)(\text{py})(\text{PPh}_3)]$ in the absence and in presence of DNA $[\text{Ru}] = 100 \mu\text{M}$, $R = 0.2, 0.4$ and 0.6 at the scan rate of 100 mVs^{-1} , in Tris-HCl buffer pH 7.1.

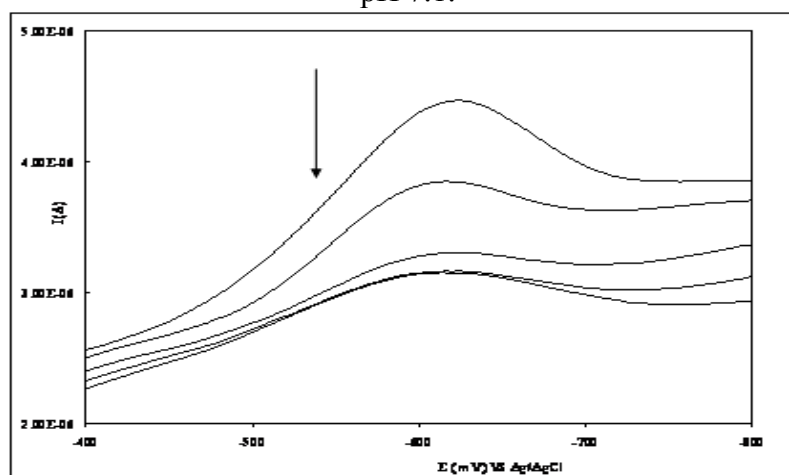
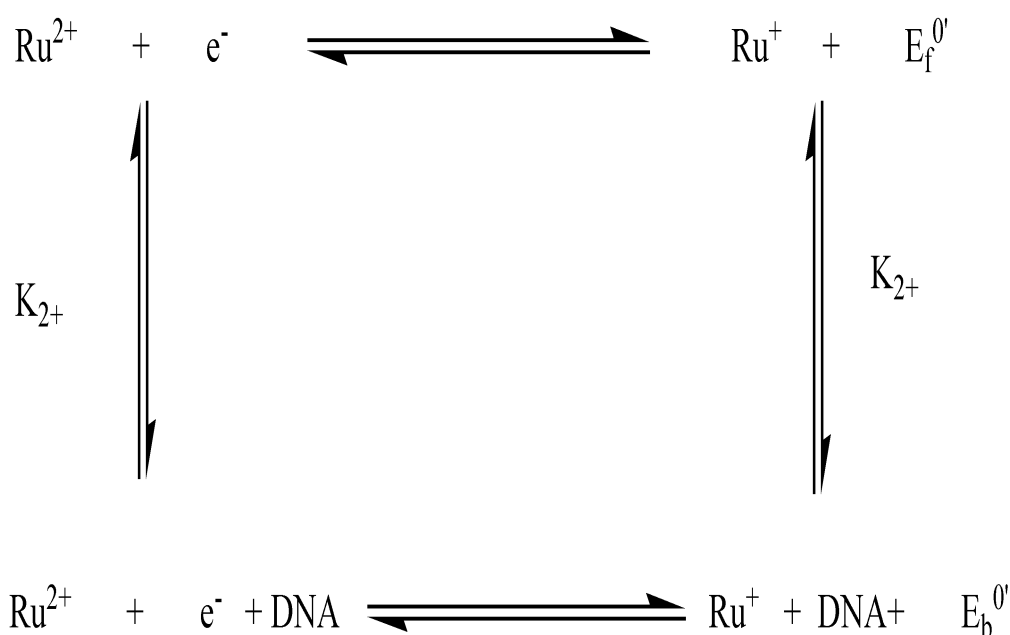


Fig. 3. Differential pulse voltammograms (DPV) of $[\text{Ru}(\text{CO})(\text{L}^1)(\text{py})(\text{PPh}_3)]$ with increasing concentration of DNA.

The formal potential E^0 (or voltammetric $E_{1/2}$), equivalent to the average of E_{pa} and E_{pc} . Upon addition of DNA, the formal potential of the complex $[\text{Ru}(\text{CO})(\text{PPh}_3)(\text{py})\text{L}^1]$ is -0.591 V in the absence of DNA undergo positive shift to -0.563 V when increasing the amount of DNA. The observed shift (28 mV) in $E_{1/2}$ values (DPV) to less negative potentials suggest that both Ru(II) and Ru(I) forms of the complex $[\text{Ru}(\text{CO})(\text{PPh}_3)(\text{py})\text{L}^1]$ bind to DNA but Ru(I) display a higher DNA binding affinity than Ru(II) form. This is illustrated by the ratio of equilibrium constants (K_+/K_{2+}) for the binding of Ru(I) and Ru(II) species to DNA.

The K_+/K_{2+} values of the complex $[\text{Ru}(\text{CO})(\text{PPh}_3)(\text{py})\text{L}^1]$ is more than unity suggesting preferential stabilization of Ru(I) form over Ru(II) form on binding to DNA. The positive shifts in formal potential indicate that complex $[\text{Ru}(\text{CO})(\text{PPh}_3)(\text{py})\text{L}^1]$ bind to DNA via intercalative mode [58]. In addition to changes in formal potential, the voltammetric peak currents decrease upon the addition of DNA to the complexes. The significant reduction in the cathodic peak current on the addition of DNA is due to slow diffusion of an equilibrium mixture of the free and DNA-bound complexes to the electrode surface [59].



Scheme 3. Estimation of the ratio of equilibrium constants for the binding of the Ru(II) and Ru(I) complexes

CD spectra

Circular dichroic spectral studies were conducted in order to determine the extent of change in conformation of DNA upon binding of complex [Ru(CO)(L¹)(py)(PPh₃)]. Circular dichroic spectral technique is useful in diagnosing changes in DNA morphology during drug-DNA interactions, as the band due to base stacking (275 nm) and that due to right-handed helicity (248 nm) are quite sensitive to the mode of DNA interactions with small molecules [61]. The changes in CD signals of DNA observed on intercalation with drugs may often be assigned to the corresponding changes in the DNA structure [62]. Thus simple groove binding and electrostatic interaction of small molecules shows less or no perturbation on the base-stacking and helicity bands. However, intercalation enhances the intensities of both the bands stabilizing the right-handed B conformation of DNA and observed for the classical intercalator methylene blue [63].

The CD spectrum of DNA was monitored in the presence of increasing amounts of complex [Ru(CO)(L¹)(py)(PPh₃)] as shown Fig 4. Upon the addition of incremental amounts of the [Ru(CO)(L¹)(py)(PPh₃)], it is observed that both the intensities of positive and negative ellipticity bands decrease. Furthermore, the positive band showed decrease in molar ellipticity with a red shift of 10 nm and the significant decrease in intensity of the DNA helicity band indicates that the DNA is unwound upon interaction with this complex [64].

These changes indicate that the structure of DNA undergoes transition from B- to A-conformation [65] This effect is attributed to intra-stand linking of adjacent guanines from the base pairs so that the DNA conformation is modified and restacking of the adjacent bases occurs. These observations clearly indicate the groove mode of binding of complexes to DNA and are not in support of the intercalative mode of binding, where the complex molecules stack in between the base pairs of DNA and thus leading to an enhancement in the positive band. The complex [Ru(CO)(L¹)(py)(PPh₃)] induces the B→A transition to a greater extent.

DNA cleavage studies by gel electrophoresis

When circular plasmid DNA is subjected to gel electrophoresis, relatively fast migration will be observed for the intact supercoil form (sc DNA or Form I). The metal complexes may cause random nicks (cuts) to one of the DNA strands if scission occurs on one strand (nicked circulus), the supercoil will relax to generate a slower-moving open circular form (oc DNA or Form II). If both strands are cleaved, a linear form (Form III) that migrates between Forms I and II will be generated [66].

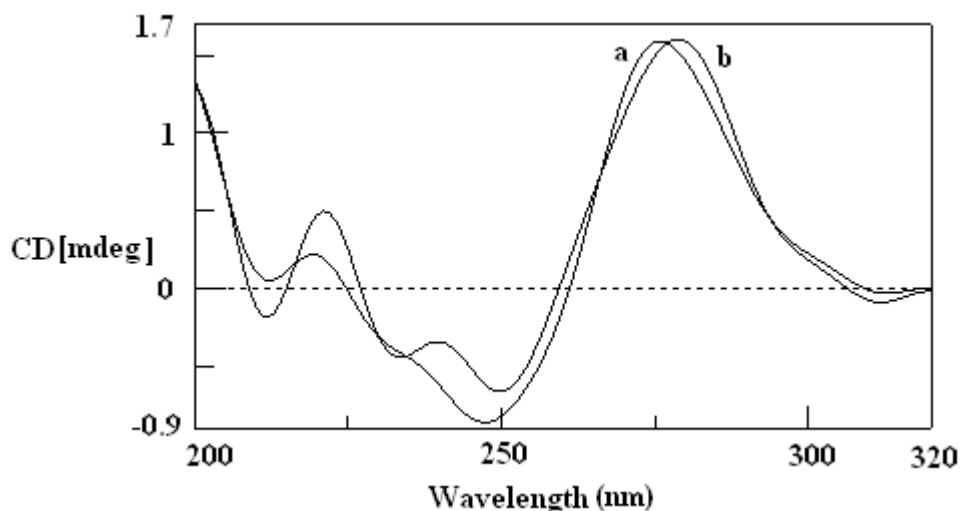


Fig. 4 Circular dichroic spectra of DNA (3.25 mM) in the absence (a) and presence (b) of $[\text{Ru}(\text{CO})(\text{L}^1)(\text{py})(\text{PPh}_3)]$ at $1/R = [\text{Ru complex}]/[\text{DNA}]$ value of 0.75.

Schematic representation of unselective cleavage on a DNA plasmid is depicted in the Fig 5. On the left, a schematic lane from an electrophoresis gel is depicted. Bands are annotated next to this lane, and the mechanism for their formation is explained on the right. The potential of the complex $[\text{Ru}(\text{CO})(\text{L}^1)(\text{py})(\text{PPh}_3)]$ to cleave DNA was studied by gel electrophoresis using supercoiled (SC) pUC18 DNA in Tris-HCl/NaCl Buffer, pH 7.2. As shown in Fig. 6, control experiments using only complex $[\text{Ru}(\text{CO})(\text{L}^1)(\text{py})(\text{PPh}_3)]$ or only H_2O_2 do not show any apparent cleavage of DNA (lanes 1-3), that is neither the complex $[\text{Ru}(\text{CO})(\text{L}^1)(\text{py})(\text{PPh}_3)]$ alone (lane 2) nor the H_2O_2 without complex (lane 3) has the cleavage activity. Only in presence of H_2O_2 the complex $[\text{Ru}(\text{CO})(\text{L}^1)(\text{py})(\text{PPh}_3)]$ converts supercoiled pUC18 DNA to a mixture of supercoiled (Form I) and nicked (Form II) DNA (lanes 4-6). Even in presence of higher concentrations of H_2O_2 the complex could cleave supercoiled form (Form I) into slower-moving open circular form (Form II) only and complete conversion into Form II and conversion of Form II to Form III was not possible. The cleavage mechanism may involve hydroxyl radical oxidative cleavage. It is evident from gel electrophoresis studies that both the complex and a co oxidant such as H_2O_2 are required to cleave plasmid DNA.

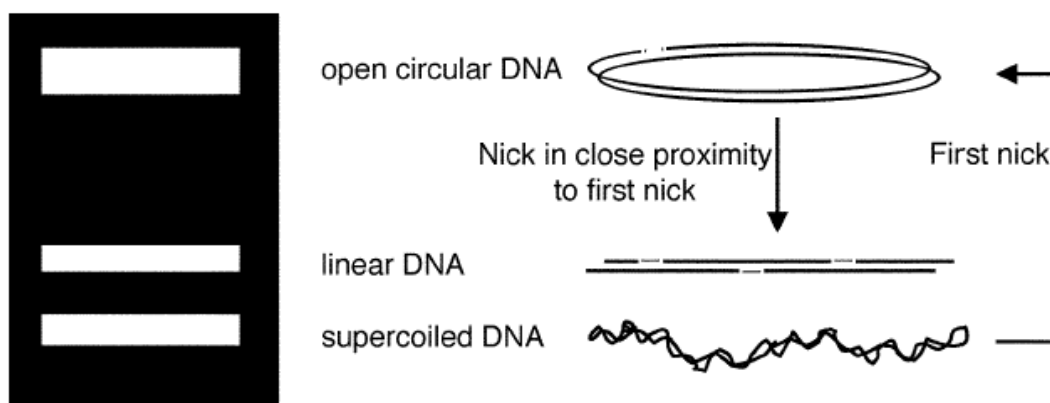


Fig. 5. Schematic representation of unselective cleavage on a DNA plasmid

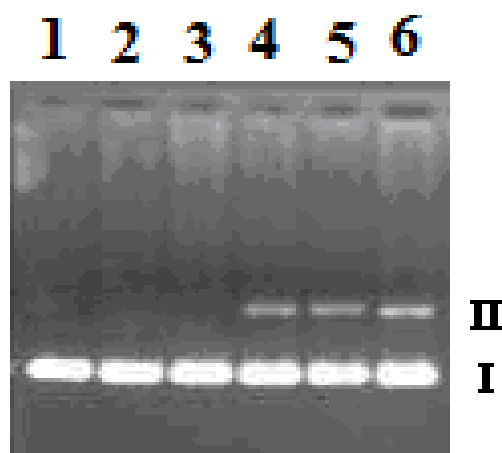
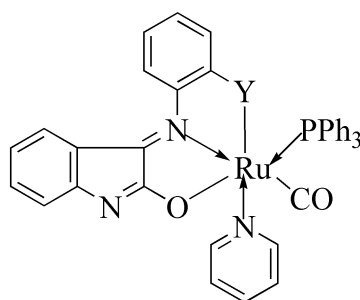


Fig. 6. Agarose gel electrophoresis diagram showing the cleavage of SC pUC18 DNA (500 ng) by complex $[\text{Ru}(\text{CO})(\text{L}^1)(\text{py})(\text{PPh}_3)]$ in Tris-HCl/NaCl Buffer (50mM, pH = 7.2) Lane 1, DNA control; Lane 2, Lane 1+ 100 μM complex; Lane 3, Lane1 + 50 μM H_2O_2 ; Lane 4, Lane1 + 100 μM complex + 50 μM H_2O_2 ; Lane 5, Lane 1 + 100 μM complex + 100 μM H_2O_2 ; Lane 6, Lane 1 + 100 μM complex + 200 μM H_2O_2 .

Conclusion

An interesting family of new six coordinated ruthenium(II) complexes incorporates with bifunctional tridentate Schiff base ligands (have been synthesized by condensing isatin with *o*-aminophenol/*o*-aminothiophenol/*o*-aminobenzoic acid in the 1:1 stoichiometric ratio in ethanolic medium). The ligands and the new complexes have been characterized by analytical, mass spectra, IR, electronic and ^1H , ^{13}C and ^{31}P -NMR studies. The redox behaviour of the complexes has been studied by cyclic voltammetry. An octahedral structure (Scheme 4) has been tentatively proposed for all the complexes. All the complexes show good catalytic and antimicrobial activity. The complex $[\text{Ru}(\text{L}^1)(\text{CO})(\text{PPh}_3)(\text{py})]$ able to bind DNA (*Herring Sperm*) with higher affinity in Ru(I) oxidation state and binding constant found by UV-Vis study is K_b is $2.1 \times 10^4 \text{ M}^{-1}$, which is less when compared with the classical intercalators. All the ruthenium(II) Schiff base complexes shows better activity in microbial studies when compared with their corresponding standards. The complex $[\text{Ru}(\text{CO})(\text{L}^1)(\text{py})(\text{PPh}_3)]$ has a tendency to cleave the DNA.



Scheme 4. Proposed structure for the new ruthenium(II) Schiff base complexes

REFERENCES

1. J.P. Tandon, K. Singh (1986) Synth. React. Inorg. Met. Org. Chem: vol 16, 1341.
2. S. Arunachalam, N. Padma Priya, K. Boopathi, C. Jayabalakrishnan, V. Chinnusamy (2010) Appl. Organomet. Chem: vol 24, 491.
3. L.D. Dave, S.K. Thampy, R. Shelat (1981) J. Inst. Chem. (India): vol 169, 237.
4. H. Singh, L.D.S. Yadav, S.B.S. Mishra (1981) J. Inorg. Nucl. Chem: vol 43, 1701.
5. L. Albanus, N.E. Bjorklund, B. Gustafsson, M. Johnson (1975) Acta Pharm. Toxic Suppl: vol 26, 93.
6. M.R. Bermejo, A. Sousa, A. Garcia-Deibe, M. Maneiro, J. Sanmartin, F. Fondo (1998) Polyhedron: vol 18, 511.
7. L. Casella, M. Gullotti, P. Vigano (1986) Inorg. Chim. Acta: vol 121, 124.
8. W. Banbe, J. Fliegner, S. Sawusch, U. Schilde, E. Uhlemann (1998) Inorg. Chim. Acta: vol 269, 350.
9. D. Coucouvanis (1979) Prog. Inorg. Chem: vol 26, 301.
10. E. Kwiatkowski, M. Kwiatkowski (1980) Inorg. Chim. Acta: vol 42, 197.
11. J.P. Costes (1987) Inorg. Chim. Acta: vol 130, 17.
12. E. Kwiatkowski, M. Kwiatkowski (1984) Inorg. Chim. Acta: vol 82, 101.
13. J.P. Costes, M.I. Fernanes-Garvia (1995) Inorg. Chim. Acta: vol 237, 57.
14. P. Bindu, M.R.P. Kurup, T.R. Satyakeerty (1998) Polyhedron: vol 18, 321.
15. V. Chinnusamy, K. Natarajan (1993) Synth. React. Inorg. Met. Org. Chem: vol 23, 889.
16. R.J.P. Williams (1990) Biochem. Soc. Trans: vol 18, 689.
17. G. Wilkinson (1987) Comprehensive Coordination Chemistry, Pergamon, Oxford: 494.
18. J. Cotamagana, J. Vargas, R. Latorre, A. Alvarado, G. Mena (1992) Coord. Chem. Rev: vol 119, 67.
19. Y.S. Pey, H.N. Pey, P. Mathur (1994) Polyhedron: vol 13, 3111.
20. R.E. Siecker, L.C. Jensen, J. Saunders-Lochr (1981) Nature (London): vol 291, 263.
21. H.A.O. Hill (1979) Adv. Inorg. Biochem: vol 1, 199.
22. R.D. Jones, D.A. Summerville, F. Basolo (1979) Chem. Rev: vol 79, 148.
23. D.M. Kurtz, D.W. Shriver, I.M. Klotz (1977) Coord. Chem. Rev: vol 24, 145.
24. M.S. Hodgson, K.O. Eccles, T.K. Lontie (1981) J. Am. Chem. Soc: vol 103, 984.
25. P. K. Bhattacharya, J. K. Barton (2001) J. Am. Chem. Soc: vol 123, 8649.
26. C. Liu, M. Wang, T. Zhang, H. Sun (2004) Coord. Chem. Rev: vol 248, 147.
27. M. Gielen, E.R.T. Tiekink (Eds. 2005), Metallotherapeutic Drugs, Metal Based Diagnostic Agents: The Use of Metals in Medicine, Wiley New York.
28. P. Uma Maheswari, V. Rajendiran, M. Palani,avar, R. Thomas, G. U. Kulkarni (2006) Inorg. Chim. Acta: vol 359, 4601.
29. Mudasir, K. Wijaya, E. T. Wahyuni, H. Inoue, N. Yoshioka (2007) Spectrochim. Acta Part A: vol 66, 163.
30. C. Tu, X. Wu, Q. Liu, X. Wang, Q. Xu, Z. Guo (2004) Inorg. Chim. Acta: vol 357, 95.
31. H. Chao, L. N. Ji (2005) Bioinorg. Chem. Appl: vol 3, 15.
32. S. Gopinathan, I.R. Unny, S. Deshphe, C. Gopinathan (1986) Ind. J. Chem. A: vol 25, 1015.
33. S. Arunachalam, N. Padma Priya, C. Jayabalakrishnan, V. Chinnusamy (2009) Spectrochim. Acta Part A: vol 74, 591.
34. S. Manivannan, R. Prabhakaran, K.P. Balasubramanian, V. Dhanabal, R. Karvembu, V. Chinnusamy, K. Natarajan (2007) Appl. Organomet. Chem: vol 21, 952.
35. R.C. Maurya, P. Patel, S. Rajput (2003) Synth. React. Inorg. Met. Org. Chem: 23, 817.
36. K.N. Kumar, R. Ramesh (2004) Spectrochim. Acta Part A: vol 60, 2913.
37. N. Dharmaraj, P. Vishwanathamorthy, P.K. Suganthy, K. Natarajan (1998) Trans. Met. Chem: vol 22, 129.
38. R. Ramesh, M. Sivagamasundari (2003) Synth. React. Inorg. Met. Org. Chem: vol 33, 899.

39. A.B.P. Lever, Inorganic Electronic Spectroscopy, 2nd edn (1984) Elsevier, New York.
40. K. ChiChak, U. Jacquenard, N.R. Branda (2002) Eur. J. Inorg. Chem: vol 2002, 357.
41. K. Natarajan, R.K. Poddar, C. Agarwala (1977) J. Inorg. Nucl. Chem: vol 39, 431.
42. L.D. Field, B.A. Messerle, L. Soler, I.E. Buys, T. Hambley (2001) J. Chem. Soc. Dalton Trans: 1959.
43. M.S. El Shahawi, A.F. Shoair (2004) Spectrochim. Acta A: vol 60, 121.
44. C. Jayabalakrishnan, R. Karvembu, K. Natarajan (2002) Trans. Met. Chem: vol 27, 790.
45. M. Muthu Tamizh, K. Mereiter, K. Kirchner, B.R. Bhat, R. Karvembu (2009) Polyhedron: vol 28, 2157.
46. N. Dharmaraj, P. Viswanathamurthi, K. Natarajan (2001) Trans. Met. Chem: vol 26, 105.
47. C.S. Allardyce, P.J. Dyson, D.J. Ellis, P.A. Salter (2003) J. Organomet. Chem: vol 668, 35.
48. B.G. Tweedy (1964) Phytopathology: vol 55, 910.
49. F. Q. Liu, Q. X. Wang, K. Jiao, F. F. Jian, G. Y. Liu, R. X. Li (2006) Inorg. Chim. Acta: vol 359, 1524.
50. D. Lawrence, V. G. Vaidyanathan, B. Unni Nair (2006) J. Inorg. Biochem: vol 100, 1244.
51. J. L. Tian, L. Feng, W. Gu, G. J. Xu, S.P. Yan, D. Z. Liao, Z. H. Jiang, P. Cheng (2007) J. Inorg. Biochem: vol 101, 196.
52. E. Kikuta, N. Katsube, E. Kimura (1999) J. Biol. Inorg. Chem: vol 4, 431.
53. L. F. Tan, X. H. Liu, H. Chao, L.N. Ji (2007) J. Inorg. Biochem: vol 101, 56.
54. P. Tamil Selvi, M. Palaniandavar (2004) Inorg. Chim. Acta: vol 337, 420.
55. S. Mahadevan, M. Palaniandavar (1998) Inorg. Chem: vol 37, 693.
56. Y. Baba, C. L. Beatty, A. Kagemoto, C. Jr. Gebelein, Eds. In Biological Activity of Polymers; ACS Symposium Series 186 (1982); American Chemical Society: Washington, DC, Chapter 14, pp 177-189.
57. X. Lu, K. Zhu, M. Zhang, H. Liu, J. Kang (2002) J. Biochem. Biophys. Methods: vol 52, 189.
58. E. M. Boon, J. K. Barton (2003) Bioconjugate Chem: vol 14, 1140.
59. S. Mahadevan, M. Palaniandavar (1996) Bioconjugate Chem: vol 7, 138.
60. M. T. Carter, M. Rodriguez, A. J. Bard (1989) J. Am. Chem. Soc: vol 111, 8901.
61. V. I. Ivanov, L. E. Minchenkova, A. S. Schyolkina, A. I. Poletayer (1973) Biopolymers: vol 12, 89.
62. P. Lincoln, E. Tulite, B. Norden (1997) J. Am. Chem. Soc: vol 119, 1454.
63. B. Norden, F. Tjerneld (1982) Biopolymers: vol 21, 1713.
64. P. Uma Maheswari, M. Palaniandavar (2003) J. Inorg. Biochem: vol 98, 219.
65. A. K. Patra, M. Nethaji, A. R. Chakravarty (2007) J. Inorg. Biochem: vol 101, 233.
66. J. K. Barton, A. L. Raphael (1984) J. Am. Chem. Soc: vol 106, 2466.